Mathematical and Computer Modelling of Dynamical Systems 1387-3954/01/0701-0001$16.00
2001, Vol. 7, No. 1, pp. 1–33

Mathematical Modelling of Diesel-Electric Propulsion Systems for Marine Vessels

JAN FREDRIK HANSEN[1,3], ALF KÅRE ÅDNANES[1] and THOR I. FOSSEN[2]

ABSTRACT

This article presents a mathematical model of a complete diesel-electric propulsion system, including components as diesel generators, distribution network, variable speed thruster-drives, and conventional motor loads. The model is split into two parts: One power generating part where the load is specified with an aggregated active and reactive power load demand. Secondly, a power consumption part where the effects of the different load types as thruster drives, motors and other loads are modelled. The model is written in a state-space form suitable for the purpose of simulation and control design. PID-controllers represent speed governors and automatic voltage regulators.

Keywords: marine systems, electrical propulsion, power, thruster drives, state space models, simulation.

1 INTRODUCTION

Electric propulsion systems are found to be beneficial in several ship applications with a varying velocity profile, such as supply vessels, floating production vessels, drill-ships, shuttle-tankers, ice-breakers, naval ships and cruise liners. Description of different kind of configurations, applications, maintenance, safety and class rules and regulations can be found in [1, 2, 3,] and [4].

[1]ABB Industry AS, P.O. Box 6540 Rodelokka, N-0501 Oslo, Norway
[2]Department of Engineering Cybernetics, Norwegian University of Science and Technology, Trondheim, Norway
[3]Corresponding author. Tel.: + 47 22 87 2627; Fax: +47 22 35 3680; E-mail: jan-fredrik.hansen@no.abb.com

The basic idea with such systems is to replace the main diesel propulsion engines with electric motors, and split the power production into several smaller diesel-generators. Electrical motors can be designed with a very high efficiency throughout the whole range of operation with respect to both speed and power output, in contrast to the diesel engine which has a clear peak in efficiency around its nominal working point. A ship which varies its velocity will be able to operate with a high efficiency for the whole range of operation by selecting the optimal number of diesel generators to supply the desired power demand. For a conventional system with diesel propulsion the efficiency would decrease noticeably for operation outside nominal operation. In addition there are several other advantages which are discussed later in this section.

In [5], [6] and [7] descriptions of systems and strategies implemented on actual ships are given. Integrated systems are discussed in [8] and [9] which describes all the electrical equipment as an integrated part of a marine system. [10], [11] and [12] describe electrical propulsion systems with a view of different kind of ships, operational profiles and propulsion motor drives. [13] and [14] describes different approaches for analysis and simulation of electric propulsion systems.

The main motivation for modelling a Diesel-Electric Propulsion (DEP) system is for simulation of different scenarios to check for performance and stability in the electrical network, and improving the Power Management System (PMS) with more advanced control theory, both for fuel optimization and increased safety. To take full advantage of the fuel saving prospect an optimization algorithm may be used to find the optimal number of generators and the optimal load sharing. For control of large load changes some type of optimal control theory could be suitable. This may necessitate a non-linear mathematical model in a compact vector form.

In [15], [16], [17] and [18] modelling, simulation and control of power plants and power systems are shown. Further a lot of attention have been paid to the stability analysis and non-linear control of Single Machine Infinite Bus systems and Multi-machine Systems in a power grid, see for example [19] and [20]. In a marine power system there are no stiff voltages, and distances are small which means that network impedances may be neglected.

In this paper well known models for each components are used and put together taking into account that there is no infinite bus. A dynamic model of the power generation system is presented and static models of the thruster drives are included. PID controllers are implemented to represent the speed

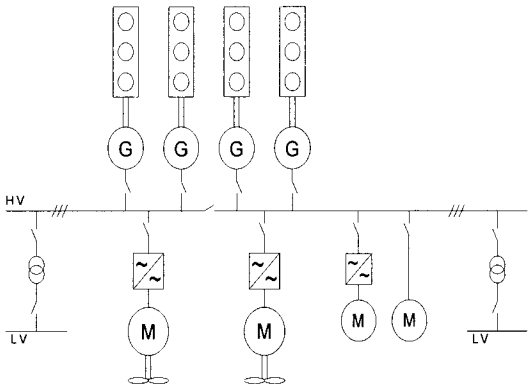

Fig. 1. A typical configuration of a diesel electric propulsion system, with diesel-generator sets, variable speed thruster drives, conventional motor loads and a low voltage distribution network.

governors and Automatic Voltage Regulators (AVR). Further the overall model is derived in a non-linear state-space form suitable for the purpose of simulation and control design.

1.1 System Description

Figure 1 shows a configuration of a diesel-electric propulsion system, with some typical components. Diesel-generators with synchronous generators (typically 3–8 units) are usually used for the power production. In some cases gas turbines are used as prime movers. The generators supply the main busbar with active (P) and reactive (Q) power. This busbar is divided into two or more sections to ensure redundancy. The voltage level will vary with installed power, typically 11 kV for installed power above 20 MW. High voltage is necessary to keep short circuit currents and load currents low.

The main power consumers are usually the propulsion and thruster drives, which may be of different types. The propellers may have either fixed or variable pitch. Synchronous or asynchronous motors are used for propulsion, where the synchronous motors are used for the highest power ratings. Typically for ships like ferries or cruise-liners which have a couple of main propellers and several smaller thrusters the synchronous motor drive is used for main propulsion and asynchronous motor drives are used for thrusters. Other ships like floating production vessels with several medium sized thrusters may have asynchronous motor drives on all the thrusters. Pulse

Width Modulated (PWM) converters, Load Commutated Inverters (LCI) or cycloconverters are the mostly used converters in the thruster-drives. Theoretically all combinations of propellers, propulsion motors and converters may be used, but today the variable speed and fixed pitch thruster drives are most common and in practise the PWM-converters are used with asynchronous motors and LCI- or cycloconverters are used with the synchronous motors.

Other consumers are motor loads for pumps, drilling, etc. mostly with fixed speed or variable speed asynchronous motors, and the low voltage distribution network for auxiliaries and hotel load.

1.2 Advantages of DEP

- *Reduced fuel consumption:*
  For vessels with large variations in operative conditions, such as transit, maneuvering, dynamic positioning etc. the propulsion load is varying from very small values to nearly full installed power. By running a specified number of diesel generators at optimum for every load condition, the overall fuel consumption is reduced compared to conventional diesel propulsion, even including losses due to the additional electrical link.
- *Improved availability:*
  With electrical propulsion two or more power buses are always used which allows for sufficient power availability during fault sequences. Also the electrical propulsion motor itself has a better reliability than the conventional diesel propulsion engine.
- *Better maneuverability:*
  Using azimuthing/podded propulsion the maneuverability of the vessel is improved with faster response for turning, stopping etc.
- *Higher flexibility in terms of engine room arrangement:*
  With conventional diesel propulsion the engine room arrangement is more or less fixed with the propeller, shaft and diesel engine. The electrical propulsion motor takes less space, and the diesel generators could be placed on any suited place. This implies the possibility of noise reduction, and to use the engine room arrangement to influence the ship stability. And again the electrical motor is far more silent than a diesel engine with the same rated power.
- *Simplified maintenance:*
  With optimal running of diesel engines the need for maintenance decrease, and by using several diesel generators, maintenance can be performed for one genset and while maintaining almost normal operation.

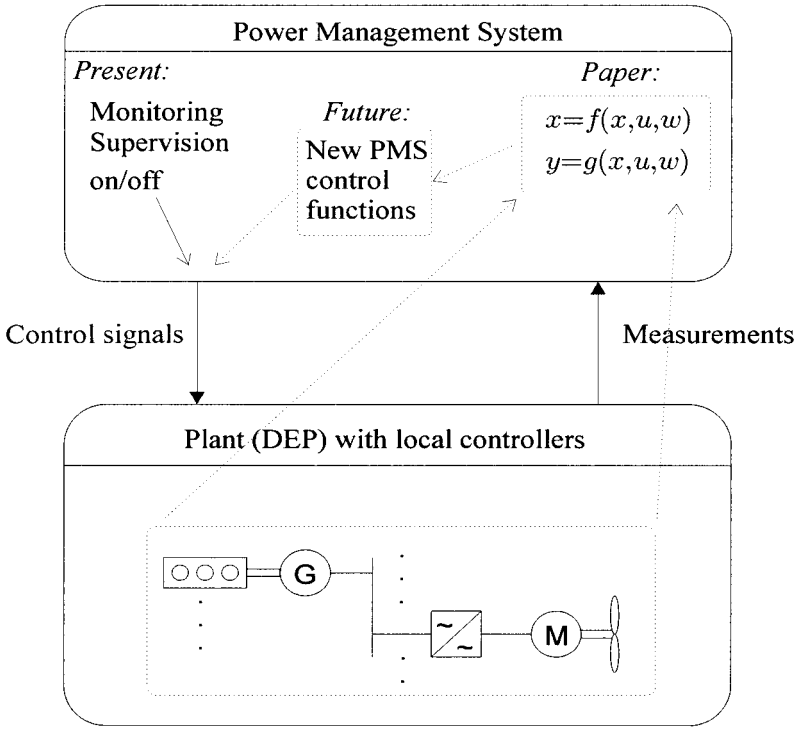

Fig. 2. Schematic overview of interaction between Power Management System and Diesel Electric Propulsion System.

Also the disadvantages should be mentioned: Introducing DEP means more components and higher investment costs, additional losses in full-load operation, other requirements/training for operational and maintenance personnel.

1.3 Modelling Specifications

A power management system (PMS) controls the operation of the DEP system. It selects how many and which generators to run, depending on the load demand from thrusters, pumps and other loads. For example when starting large loads the PMS checks the available power and decides if it is necessary to start up another diesel generator. Smaller load changes are taken care off by making sure that there always is a power reserve according to safety limits. Modelling specifications:

- The mathematical description should be general with respect to numbers of components as generators and thruster drives. Other consumers may be represented with an aggregate load.
- There should be an on/off feature for the generators and the thruster drives in order to simulate component outages.
- PMS control functions focus on power production, hence advanced dynamic models shall be used for the generators and simplified static models shall be used for thruster drives and other consumers.
- The final model shall be in a state-space vector form suitable for control design.

1.4 Outline of the Paper

The model is split into two parts, power generation and power consumption. Section 2 presents power generation modelling with diesel engines, synchronous generators, load module which represents the interconnection of the generators, speed governor and automatic voltage controllers. Well known models are used for each component, but special attention has been paid to the interconnection of several synchronous generators in the load module.

In Section 3 the power consumption is considered, modelling the thruster drives alongside other loads. This model gives the active and reactive power demand for use in the load module in Section

Section 4 presents a compact state space model suitable for simulation and control design.

Finally, some simulations are shown in Section 6 with PID-controllers for voltage and frequency stabilization.

2 POWER GENERATION

2.1 Overall Model Structure

The power generation plant consists of synchronous generators powered by medium speed diesel engines supplying a common load, and low level speed and voltage controllers (usually PID controllers).

In stiff networks an infinite busbar with fixed voltage and frequency is used as reference for the busbar voltage and the power angle. A marine power system is an isolated system and for the model presented in this paper the rotor

speed of one generator is chosen as reference and the power angles of the other generators are computed relative to this reference. The power angle of the reference generator and the busbar voltage is computed by the load module as a function of the generator currents as described in Section 2.5.

A 7th-order model is used for each of the synchronous generators, and the interconnection is made by a load module representing the total load as a variable impedance. The load module adds (vectorially) the current outputs from the generators and returns the busbar voltage depending on the load characteristic (constant impedance, constant power etc.). Electrical quantities are modelled in the two axis *dq*-frame. Simple 1st-order models are used for the diesel engines, and PID controllers represent the speed governors and Automatic Voltage Regulators (AVR). An on/off feature for each diesel-generator is included in the model for simulation of performance when connecting/disconnecting generation units. A schematic presentation of the overall model structure with input and output relationships is shown in Figure 3. The input/output variables are defined in the following subsections alongside each model description.

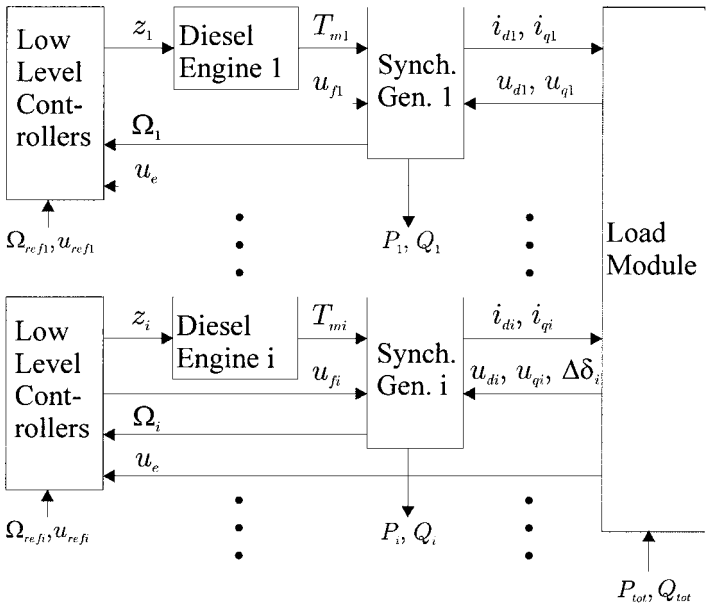

Fig. 3. Block diagram of plant model with input and output relationship.

2.2 Per-Unit Reference Frame

The model is presented with per unit variables with the rated values of the largest synchronous generator as references. That is if different sized generators are considered the parameters for the smaller generators have to be recalculated to this frame. The reference frame is defined as follows:

Phase voltage [V]: $U_{ref} = \sqrt{2/3}U_N$, where U_N is the nominal busbar voltage [V]. *Phase current [A]:* $I_{ref} = \sqrt{2}I_N$, where I_N is the nominal current [A]. *Apparent power [VA]:* $S_{ref} = 3/2U_{ref}I_{ref}$. *Electrical angular frequency [rad/s]:* $\omega_N = 2\pi f_N$, where f_N is nominal busbar frequency [1/s]. *Mechanical angular frequency [rad/s]:* $\Omega_{ref} = \omega_N/(p/2)$, where p is the pole number of the generator. *Torque [Nm]:* $T_{ref} = S_{ref}/\Omega_{ref}$.

2.3 Diesel Engines

As an approximation of the medium speed diesel engine dynamics a 1st order model is used [21].

$$\dot{T}_m = \frac{1}{T_{DE}}(-T_m + z) \tag{1}$$

where T_m is mechanical shaft torque [pu], T_{DE} is diesel dynamic time constant [s] and z is fuel-pump index [pu]. Equation (1) is scaled such that the fuel-pump index may vary between 0 and 1 ,that is from 0 to 100% capacity of the fuel-pump.

In addition a simplified non-linear function describing the specific fuel consumption (ρ [g/kWh]) is included for estimating the fuel consumption.

$$\rho = f(z) \tag{2}$$

Function f in (2) is assumed convex in $z \in [0, 1]$, with a minimum at the diesel engine rated power, usually at about 90% of maximum power.

This diesel-engine model is considered adequate for the purpose of this model where performance at the electrical side is the main subject of interest. Running conditions like air intake and exhaust temperature can not be obtained from this simplified model.

2.4 Synchronous Generators

The well known two-axis *dq*-model is used for each of the synchronous generators, and the notation from [22] is used. Differential equations describ-

ing the electrical stator-, rotor- and damper-windings dynamics are included in addition to the mechanical differential equations for the shaft speed and power angle. Magnetic saturation, hysteresis, and eddy-currents are neglected. These are assumed to have minor impact on the dynamic performance of interest here.

For each generator the model is given below with the following variables and parameters:

- *Mechanical States:*
  - $\Delta\delta$: Relative power angle referred to reference gen., that is the angle between the q-axis of the current generator and the q-axis of the reference generator.
  - Ω : Shaft speed [pu].
- *Electrical States:*
  - ψ_d : d-axis stator winding flux linkage [pu].
  - ψ_q : q-axis stator winding flux linkage [pu].
  - ψ_D : d-axis damper winding flux linkage [pu].
  - ψ_Q : q-axis damper winding flux linkage [pu].
  - ψ_f : Field winding (rotor) flux linkage [pu].
  - Inputs:
  - u_d : d-axis terminal voltage [pu].
  - u_q : q-axis terminal voltage [pu].
  - Ω_1 : Shaft speed reference generator [pu].
  - T_m : Mechanical shaft torque [pu].
  - u_f : Field voltage [pu].
  - Outputs:
  - i_d : d-axis stator current [pu].
  - i_q : q-axis stator current.[pu].
  - Ω : Shaft speed [pu].
  - $\Delta\delta$: Relative power angle referred to ref. gen.[rad].
  - P : Active power [pu].
  - Q : Reactive power [pu].
  - Parameters:
  - ω_N : Nominal electrical angular frequency [rad/s].
  - T_a : Mechanical time constant [s]. T_a equals $\Omega_{ref}\frac{J}{T_{ref}}$, where J is the total inertia.
  - r_s : Armature resistance [pu].
  - x_d : d-axis reactance [pu].

x_q : q-axis reactance [pu].
T_D : d-axis damper winding time constant [s].
T_Q : q-axis damper winding time constant [s].
T_f : Field winding time constant [s].
σ_D : 'Leakage factor' (damper/stator-winding, d-axis), non-dimensional.
σ_Q : 'Leakage factor' (damper/stator-winding, q-axis), non-dimensional.
σ_f : 'Leakage factor' (field/stator-winding), non-dimensional.
μ_D : 'Coupling factor' (damper/field-winding), non-dimensional.
μ_f : 'Coupling factor' (field/damper-winding), non-dimensional.

The electrical state equations are (voltage balance for each winding):

$$\dot{\psi}_d = \omega_N(\Omega\psi_q + i_d r_s + u_d) \tag{3a}$$
$$\dot{\psi}_q = \omega_N(-\Omega\psi_d + i_q r_s + u_q) \tag{3b}$$
$$\dot{\psi}_D = -\frac{1}{T_D} i_D \tag{3c}$$
$$\dot{\psi}_Q = -\frac{1}{T_Q} i_Q \tag{3d}$$
$$\dot{\psi}_f = \frac{1}{T_f}(-i_f + u_f) \tag{3e}$$

where the flux linkages are:

$$\psi_d = -x_d i_d + i_D + i_f \tag{4a}$$
$$\psi_q = -x_q i_q + i_Q \tag{4b}$$
$$\psi_D = -(1-\sigma_D)x_d i_d + i_D + \mu_D i_f \tag{4c}$$
$$\psi_Q = -(1-\sigma_Q)x_q i_q + i_Q \tag{4d}$$
$$\psi_f = -(1-\sigma_f)x_d i_d + \mu_f i_D + i_f \tag{4e}$$

The mechanical state equations are (rotational speed and relative power angle):

$$\dot{\Omega} = \frac{1}{T_a}(T_m - T_e) \tag{5}$$
$$\Delta\dot{\delta} = \omega_N(\Omega - \Omega_1) \tag{6}$$

where the electromagnetic torque is:

$$T_e = \psi_d i_q - \psi_q i_d \tag{7}$$

For the reference generator, defined as generator 1, $\Omega = \Omega_1$ hence $\Delta\dot{\delta}_1 = 0$.

Output equations in addition to the current outputs (i_d, i_q) and the mechanical states (Ω, $\Delta\delta$) are:

$$P = u_d i_d + u_q i_q \tag{8}$$

$$Q = u_q i_d - u_d i_q \tag{9}$$

Equations (3) and (4) can be written in a compact state-space form. Define the vectors $\boldsymbol{\psi} = [\psi_d, \psi_q, \psi_D, \psi_Q, \psi_f]^T$, $\mathbf{i} = [i_d, i_q, i_D, i_Q, i_f]^T$, $\mathbf{u}_g = [u_d, u_q]^T$ then:

$$\dot{\boldsymbol{\psi}} = \mathbf{K}(\Omega)\psi + \mathbf{R}\mathbf{i} + \mathbf{E}\mathbf{u}_g + \mathbf{b}u_f \tag{10}$$

$$\psi = \mathbf{X}\mathbf{i} \Rightarrow \mathbf{i} = \mathbf{X}^{-1}\psi \tag{11}$$

where

$$\mathbf{K}(\Omega) = \begin{bmatrix} 0 & \omega_N\Omega & 0 & 0 & 0 \\ -\omega_N\Omega & 0 & 0 & 0 & 0 \\ 0 & 0 & 0 & 0 & 0 \\ 0 & 0 & 0 & 0 & 0 \\ 0 & 0 & 0 & 0 & 0 \end{bmatrix} \mathbf{R} = \begin{bmatrix} \omega_N r_s & 0 & 0 & 0 & 0 \\ 0 & \omega_N r_s & 0 & 0 & 0 \\ 0 & 0 & -\frac{1}{T_D} & 0 & 0 \\ 0 & 0 & 0 & -\frac{1}{T_Q} & 0 \\ 0 & 0 & 0 & 0 & -\frac{1}{T_f} \end{bmatrix} \tag{12}$$

$$\mathbf{E} = \begin{bmatrix} \omega_N & 0 \\ 0 & \omega_N \\ 0 & 0 \\ 0 & 0 \\ 0 & 0 \end{bmatrix} \mathbf{X} = \begin{bmatrix} -x_d & 0 & 1 & 0 & 1 \\ 0 & -x_q & 0 & 1 & 0 \\ -(1-\sigma_D)x_d & 0 & 1 & 0 & \mu_D \\ 0 & -(1-\sigma_Q)x_q & 0 & 1 & 0 \\ -(1-\sigma_f)x_d & 0 & \mu_f & 0 & 1 \end{bmatrix} \tag{13}$$

$$\mathbf{b} = \begin{bmatrix} 0 & 0 & 0 & 0 & \frac{1}{T_f} \end{bmatrix}^T \tag{14}$$

This yields:

$$\dot{\boldsymbol{\psi}} = (\mathbf{K}(\Omega) + \mathbf{R}\mathbf{X}^{-1})\psi + \mathbf{E}\mathbf{u}_g + \mathbf{b}u_f \tag{15a}$$

$$\dot{\Omega} = \frac{1}{T_a}(T_m - h(\psi)) \tag{15b}$$

$$\Delta\dot{\delta} = \omega_N(\Omega - \Omega_1) \tag{15c}$$

where $h(\boldsymbol{\psi})$ is given by (7). Further define $\boldsymbol{\psi}_s = [\psi_d, \psi_q]^T$ and $\mathbf{i}_s = [i_d, i_q]^T$ which are the reduced flux-linkage and current vectors containing only stator quantities (subscript s). Then

$$h(\psi) = \boldsymbol{\psi}_s^T \mathbf{H}\mathbf{i}_s = \boldsymbol{\psi}^T(\mathbf{G}^T\mathbf{H}\mathbf{G})\mathbf{X}^{-1}\boldsymbol{\psi} \tag{16}$$

where

$$\mathbf{H} = \begin{bmatrix} 0 & 1 \\ -1 & 0 \end{bmatrix}, \mathbf{G} = \begin{bmatrix} 1 & 0 & 0 & 0 & 0 \\ 0 & 1 & 0 & 0 & 0 \end{bmatrix} \tag{17}$$

$$\mathbf{G}^T\mathbf{H}\mathbf{G} = \begin{bmatrix} 0 & 1 & 0 & 0 & 0 \\ -1 & 0 & 0 & 0 & 0 \\ 0 & 0 & 0 & 0 & 0 \\ 0 & 0 & 0 & 0 & 0 \\ 0 & 0 & 0 & 0 & 0 \end{bmatrix} \tag{18}$$

and $c = x_d\big(\mu_f\mu_D - \mu_f + \mu_f\sigma_D - \mu_D + 1 - \sigma_D + \sigma_f\mu_D - \sigma_f\big)$. The outputs are then $\mathbf{i}_s$, P and Q:

$$\mathbf{i}_s = \mathbf{G}\mathbf{X}^{-1}\boldsymbol{\psi} \tag{19}$$

$$P = \mathbf{u}_g^T\mathbf{i}_s = \mathbf{u}_g^T\mathbf{G}\mathbf{X}^{-1}\boldsymbol{\psi} \tag{20}$$

$$Q = -\mathbf{u}_g^T\mathbf{H}\mathbf{i}_s = -\mathbf{u}_g^T\mathbf{H}\mathbf{G}\mathbf{X}^{-1}\boldsymbol{\psi} \tag{21}$$

To summarize the state space model representing one generation unit is:

$$\dot{\boldsymbol{\psi}} = (\mathbf{K}(\Omega) + \mathbf{R}\mathbf{X}^{-1})\boldsymbol{\psi} + \mathbf{E}\mathbf{u}_g + \mathbf{b}u_f \tag{22a}$$

$$\dot{\Omega} = \frac{1}{T_a}(T_m - \boldsymbol{\psi}^T(\mathbf{G}^T\mathbf{H}\mathbf{G})\mathbf{X}^{-1}\boldsymbol{\psi}) \tag{22b}$$

$$\Delta\dot{\delta} = \omega_N(\Omega - \Omega_1) \tag{22c}$$

2.5 Load Module

In this section the function $\mathbf{u}_g$ from (22) is found.

The load module represents the interconnection of the generators (main busbar) by computing the generators terminal voltage as a function of load characteristics. In [23] several types of load modelling are discussed. Two static load models are considered in this paper, an approximation for constant power and constant impedance.

The constant impedance load type will represent the passive loads as distribution network and hotel loads while the approximated constant power load type will represent the variable speed drives. An aggregate load is used for each type.

Frequency dependence and load dynamics are neglected. This is based on the assumptions that the frequency will be close to nominal value, and the load demand is modelled as a quasi-stationary load described in the next section.

This module consists of algebraic equations taking the generator currents and total active and reactive power demand as inputs, and giving generator terminal voltage as output. The currents are summarized and the busbar voltage is computed by multiplying with the equivalent load impedance.

- *Inputs:*
  - i_{di} : d-axis phase current generator i [pu].
  - i_{qi} : q-axis phase current generator i [pu].
  - $\Delta\delta_i$: Relative power angle (see Figure 4) referred to gen. no.1[rad].
  - P_Z : Active power demand, const. impedance [pu].
  - Q_Z : Reactive power demand, const. impedance [pu].
  - P_S : Active power demand, const. power [pu].
  - Q_S : Reactive power demand, const. power [pu].
- *Outputs:*
  - u_{di} : d-axis terminal voltage generator i [pu].
  - u_{qi} : q-axis terminal voltage generator i [pu].

The load impedance for the constant impedance load type is computed from (23) for unity busbar voltage. The 'constant impedance' term means that the load impedance is kept constant for constant power demand and not dependent of the busbar voltage.

$$z_Z = \left(\frac{1}{P_Z + jQ_Z}\right)^* \tag{23}$$

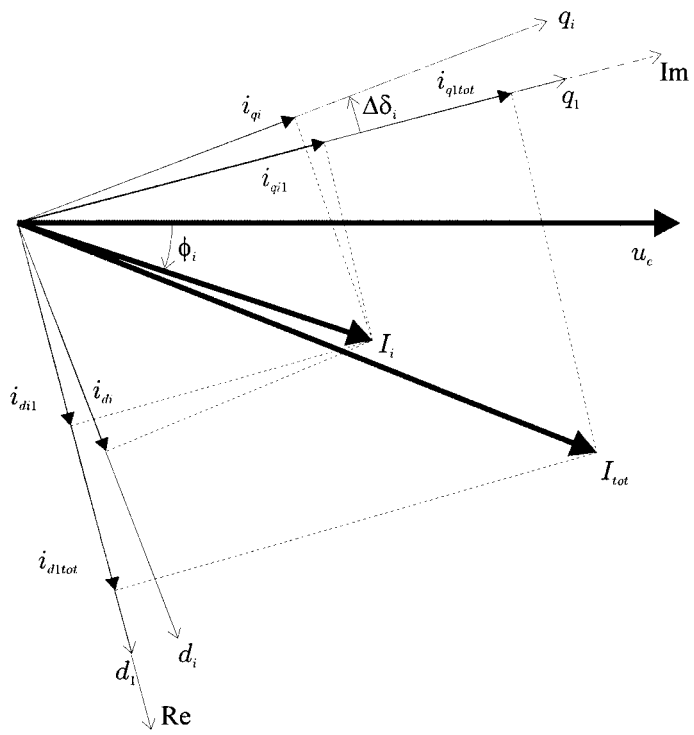

Fig. 4. Phasor diagram showing transformation of current unit *i* to the *dq* frame of unit 1.

where * denotes the complex conjugate. The load impedance for the ideal constant power load type is computed from (24).

$$z_S = \left(\frac{|u_{di} + ju_{qi}|^2}{P_S + jQ_S} \right)^* \tag{24}$$

This would have to be solved by iteration since the busbar voltage is a function of the load impedance. Besides slowing down simulation the busbar voltage would initially increase for positive step in the power demand. This is not the case for the thruster drives where the voltage drops for increasing load and then tends to draw constant power by increasing load current for decreasing voltage. As an approximation for this the voltage from the previous simulation step is used in (24), though filtered through a first order transfer function with a small time constant (0.01 s) for avoiding numerical difficulties with a step

change in impedance for each simulation step. The equivalent load impedance is then computed as a parallel connection of the two impedances.

$$z_{eq} = (r_{eq} + jx_{eq}) = \frac{z_Z z_S}{z_Z + z_S} \tag{25}$$

The currents are given in the individual *dq* frames of each generator, and before summation they are transformed to the *dq*-frame of the reference generator as shown in Figure 4.

$$I_{Gi} = (i_{di} + ji_{qi})e^{j(\Delta\delta_i)} \tag{26}$$

$$I_{tot} = (i_{dtot} + ji_{qtot}) = I_{G1} + I_{G2} + ... + I_{Gn} \tag{27}$$

where n is the number of generators connected to the busbar. The busbar voltage and the transformation for the individual generators are given by (28).

$$u_{d1} = r_{eq}i_{dtot} - x_{eq}i_{qtot} \tag{28a}$$

$$u_{q1} = r_{eq}i_{qtot} + x_{eq}i_{dtot} \tag{28b}$$

$$(u_{di} + ju_{qi}) = (u_{d1} + ju_{q1})e^{-j(\Delta\delta_i)} \tag{28c}$$

To write these equations in a compact vector form with real quantities note that the transformation of vectors between orthogonal coordinate systems with an angle difference φ is:

$$\Phi(\varphi) \triangleq \begin{bmatrix} \cos(\varphi) & -\sin(\varphi) \\ \sin(\varphi) & \cos(\varphi) \end{bmatrix} \tag{29}$$

$$\Phi(-\varphi) = \Phi^{-1}(\varphi) = \Phi^T(\varphi) \tag{30}$$

Define $\mathbf{i}_{tot} = [i_{dtot}, i_{qtot}]^T$ referred to *dq* axis of the reference generator. Then

$$\mathbf{i}_{tot} = \mathbf{i}_{s1} + \Phi(\Delta\delta_2)\mathbf{i}_{s2} + ... + \Phi(\Delta\delta_n)\mathbf{i}_{sn} \tag{31}$$

and the busbar voltage:

$$\mathbf{u}_{g1} = \mathbf{Z}\mathbf{i}_{tot} \tag{32}$$

$$\mathbf{u}_{g2} = \Phi^T(\Delta\delta_2)\mathbf{Z}\mathbf{i}_{tot} \tag{33}$$

$$. \tag{34}$$

$$. \tag{35}$$

$$. \tag{36}$$

$$\mathbf{u}_{gn} = \Phi^T(\Delta\delta_n)\mathbf{Z}\mathbf{i}_{tot} \tag{37}$$

where

$$\mathbf{Z} = \begin{bmatrix} r_{eq} & -x_{eq} \\ x_{eq} & r_{eq} \end{bmatrix} \tag{38}$$

2.6 Speed Governor and Automatic Voltage Regulator

PID controllers are representing the speed governors and automatic voltage regulators. Due to parallel controlling of busbar frequency (generator speeds) and voltage, special consideration has to be taken for inclusion of integral effect in all units. This will lead to an arbitrary load sharing due to variations in parameters between the units. Several control strategies may be considered:

- Parallel PID controllers with droop, that is a steady state offset in the controlled variables is introduced, but desired load sharing is achieved.
- Parallel PID controllers where one generator controls the frequency and voltage, and the other controls delivered active and reactive power with the set-points taken from the delivered power of the first generator. This will ensure equal load sharing.
- One generator with integral action, and the other with proportional control. This means only one generator will automatically take all the load change while the other will deliver constant power depending on a bias signal to the reference. This may yield large unexpected load differences for the generators when the total load is highly varying.
- Same as previous, but with a load sharing unit providing the proportional controlled generators with a bias signal taken from the deviation between the power from generator with integral action and the current one. This would lead to equal load sharing.

For the simulations in this paper the latter control strategy is implemented when equal load sharing is desired.

The PID controllers are implemented in a standard form (39):

$$u = K_p \left(e + \frac{1}{T_i} \int_0^t e(\tau) d\tau + T_d \dot{e} \right) \tag{39}$$

hence

$$\dot{u} = K_p \left(T_d \ddot{e} + \dot{e} + \frac{1}{T_i} e \right) \tag{40}$$

where u is control input to the plant (fuel index or field voltage), e is deviation from set points (gen. speed or voltage). K_p, T_i and T_d are gain, integral time and derivative time respectively. Notice that by setting $T_d = 0$ and/or $T_i = \infty$ (or as high as possible) the controller can be chosen as PID−, PI−, PD− or P− type.

3 POWER CONSUMPTION

This second part of the system modelling is a description of the different power consumers in a diesel-electric propulsion system with special attention to the variable speed thruster drives. This part computes the active and reactive power demand for each load and sets up an aggregate load of both constant impedance and constant power types to be used in the previous part. For each load there are several components, and the idea is to specify a power demand at the end of the consumer line and add up power losses and finally get the power demand at the busbar. In this paper only static models are considered because the load dynamics are assumed to have minor impact on the power generation part with the chosen model strategy by specifying an active and reactive power demand. Dynamic models may be considered in future work for improving the accuracy of the load models.

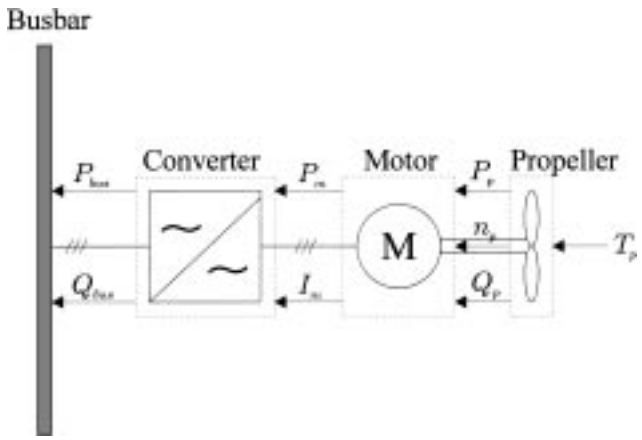

Fig. 5. Schematic diagram of the variable speed thruster drive with inputs and outputs for modelling.

3.1 Thruster Drives

Different kind of thruster drives may be considered. In this paper is the variable speed thruster drive is used which consists of a propeller, shaft, propulsion motor and a frequency converter. For the largest drives ($>$5–8 MW, dependent on vendor strategy, gearing etc.) synchronous motors may be used with either cycloconverter or LCI (Load Commutated Inverter) – converter. For the smaller drives asynchronous motors with PWM (Pulse Width Modulated) converters are more suitable. The propellers of the variable speed thruster drives have usually fixed pitch. The variables are scaled according to Section 2.2 to fit the power production part. Figure 5 shows the relationship between the different blocks and defines the inputs and outputs.

3.1.1 Propeller

For a fixed pitch propeller the relationship between thrust force, torque and power can be established [21]:

$$T_p = \rho D^4 K_T n|n| \tag{41}$$

$$Q_p = \rho D^5 K_Q n|n| \tag{42}$$

$$P_p = \frac{2\pi}{60} n Q_p \tag{43}$$

where T_p is propeller thrust [N], n is propeller shaft speed [r/min] Q_p is propeller torque [Nm] and P_p is propeller power [W]. The parameters are: ρ – water density, D – propeller diameter, K_T – thrust coefficient, K_Q – torque coefficient. Rearranging (41)–(43) yields:

$$n = \text{sign}\left(\frac{T}{\rho D^4 K_T}\right)\sqrt{\left|\frac{T}{\rho D^4 K_T}\right|} \tag{44}$$

$$Q_p = \frac{D K_Q}{K_T} T \tag{45}$$

$$P_p = \text{sign}\left(\frac{T}{\rho D^4 K_T}\right)\sqrt{\left|\frac{T}{\rho D^4 K_T}\right|} \tag{46}$$

K_Q and K_T are varying parameters and the characteristics also change between different propeller types. For simplicity they are chosen as positive constants

in the simulations in this paper. (46) can then be written as:

$$P_p = k \cdot \text{sign}(T) T \sqrt{|T|} \tag{47}$$

where $k = 1/\sqrt{(\rho D^4 K_T)^3}$.

3.1.2 Propulsion motors

Either synchronous motors or asynchronous motors are used for propulsion. In this section a loss model for each type is presented. The equations are based on [24], [25] and [26]. The inputs from the propeller model are:

- n_p: propeller shaft speed [pu].
- Q_p: propeller mechanical shaft torque [pu].
- P_p: propeller shaft power [pu].

Synchronous Motor:

Synchronous motor losses are simplified to four terms, the electrical rotor and stator losses, core losses which are assumed to be proportional to the square of the air gap voltage, and friction losses.

$$P_{loss,\ synch} = r_f i_f^2 + r_a i_a^2 + \frac{e_{ag}^2}{r_{ms}} + k_{f_1} n_p \tag{48}$$

where r_f and i_f are field winding resistance and current, r_a and i_a are armature winding resistance and current, r_{ms} is equivalent core loss resistance, e_{ag}^2 is air gap voltage and k_{f_1} is friction constant. It is further assumed that the armature current is proportional to the electromechanical torque and air gap voltage is proportional to shaft speed, hence:

$$\begin{aligned} i_a = k_1 Q_p &\Longrightarrow k_1 = \frac{i_{aN}}{Q_{pN}} \\ e_{ag} = k_2 n_p &\Longrightarrow k_2 = \frac{e_{agN}}{n_{pN}} \end{aligned} \tag{49}$$

Field current i_f is for simplicity assumed to be:

$$i_f = k_3 + k_4 i_a = k_3 + k_4 k_1 Q_p \tag{50}$$

The constant k_3 represent the idle speed excitation and k_4 approximates excitation due to load variation. These constants should be chosen to fit

characteristic motor data. Subscript N denotes *Nominal* values. This yields:

$$P_{loss,\,synch} = r_f i_f^2 + k_5 Q_p^2 + k_6 n_p^2 + f_r n_p \tag{51}$$

$$P_m = P_p + P_{loss,\,synch} \tag{52}$$

$$I_m = k_1 Q_p \tag{53}$$

where $k_5 = k_1^2 r_a$, $k_6 = k_2^2 / r_{ms}$.

Asynchronous Motor: Asynchronous motor losses are simplified to four terms: the electrical stator and rotor losses, core losses and mechanical friction losses.

$$P_{loss,\,asynch} = r_r i_r^2 + r_s i_s^2 + \frac{e_{ag}^2}{r_{ma}} + k_{f_2} n_p \tag{54}$$

where r_r is rotor resistance, r_s is stator resistance, r_{ma} is magnetizing resistance and k_{f2} is friction coefficient. The following assumptions are made for the asynchronous motor:

- Control strategy is assumed to keep air gap flux constant, hence $i_m = i_{mN}$.
- Slip frequency is small compared to synchronous frequency.
- Slip frequency is proportional to load torque.
- Hysteresis and saturation are neglected.

Hence:

$$e_{ag} = k_7 n_s \Longrightarrow k_7 = \frac{e_{aN}}{n_{sN}} \tag{55}$$

$$n_s = n_{sl} + n_p \tag{56}$$

$$n_{sl} = k_8 Q_p \Longrightarrow k_8 = \frac{n_{slN}}{Q_{pN}} \tag{57}$$

$$i_r = k_9 Q_p \Longrightarrow k_9 = \frac{i_{rN}}{Q_{pN}} \tag{58}$$

$$i_s^2 = i_r^2 + i_m^2 \tag{59}$$

$$i_m = i_{mN} = k_{10} \tag{60}$$

Subscript N denotes *Nominal* values. This yields:

$$P_{loss,\,asynch} = k_{11}Q_p^2 + k_{12} + (k_{13}Q_p + k_{14}n_p)^2 + k_{f_2}n_p \tag{61}$$

$$P_m = P_p + P_{loss,\,asynch} \tag{62}$$

$$I_m = (k_7 Q_p)^2 + k_{10} \tag{63}$$

where $k_{11} = (r_r + r_s)k_9^2$, $k_{12} = r_s k_{10}^2$, $k_{13} = k_7 k_8/\sqrt{r_{ma}}$ and $k_{14} = k_7/\sqrt{r_{ma}}$.

3.1.3 Converters

Two types of converters are considered, the cycloconverter and the PWM converter. The loss models are based on [26].

Cycloconverter: The conduction losses are assumed to be dominating and a loss model suitable for curve fitting of characteristics is given in (64).

$$P_{loss,cyclo} = P_0 + k_{15}I_m + k_{16}I_m^2 \tag{64}$$

where I_m is the motor current given by (53), and P_0 is a term representing possible reverse recovery losses, cooling losses etc. and k_{15} and k_{16} are constants representing conduction losses. The cycloconverter is usually combined with a synchronous motor in the thruster drives. The output power factor is then controlled to unity, hence the power factor at the network then mostly depends on the firing angle of the cycloconverter. This will vary slightly with different configurations, but mainly the converter has a maximum power factor (0.7–0.75) for loads from 50–100%. For lower loads the power factor is assumed to decrease linearly.

$$PF = PF_{\max}, \qquad P_m > P_{PF\max} \tag{65}$$

$$PF = PF_{\min}, \qquad P_m < P_{PF\min} \tag{66}$$

$$PF = P_{PF\min} + \frac{PF_{\max} - PF_{\min}}{P_{PF\max} - P_{PF\min}}(P_m - P_{PF\min}),$$
$$P_{PF\min} < P_m < P_{PF\max} \tag{67}$$

where PF denotes power factor, P_{PF} denotes load power at certain PF and P_m is the load power. The PF_{min} factor is used to avoid numerical difficulties around zero power and can be chosen as low as possible according to this.

$$P_{bus} = P_m + P_{loss,cyclo} \tag{68}$$

$$Q_{bus} = \sqrt{\left(\frac{P_{bus}}{PF}\right)^2 - P_{bus}^2} \tag{69}$$

PWM-converter: The power losses of the PWM-converter are assumed to be dominated by switching losses, conduction losses and cooling and power supply to the control circuit losses. A general loss model suitable for curve fitting of characteristics is given in (70).

$$P_{loss,\,PWM} = P_0 + k_{17} I_m + k_{18} I_m^2 + k_{19} P_m + k_{20} P_m^2 \tag{70}$$

where I_m is the motor current given by (63), P_0 represents auxiliary power and cooling losses, and P_m is load power. Switching losses are included in k_{17}, inverter conducting losses are included in k_{17} and k_{18} and rectifier conducting losses are included in k_{19} and k_{20}. The power factor PF may be assumed to vary linear with load power, from 1,0 at no-load to 0,95 at full load.

$$P_{bus} = P_m + P_{loss,PWM} \tag{71}$$

$$Q_{bus} = \sqrt{\left(\frac{P_{bus}}{PF}\right)^2 - P_{bus}^2} \tag{72}$$

3.2 Other Loads

Other loads may be different kind of motor loads for pumps, compressors etc., and the low voltage distribution network for hotel load and other low voltage power consumers. An aggregate load is considered specifying active and reactive load demand.

4 RESULTING STATE-SPACE MODEL

In this section the power production part is written in compact vector form as a non-linear state-space model. The power production part consists only of algebraic equations and hence act as disturbance with the active and reactive load power demand. Further the state-space model is written in open loop, without the speed governors and voltage regulators. The purpose of writing the model this way is for introducing advanced control theory for supervisory control schemes in the power management system. Using the same notation and vector definitions as in Section 2 the state equations for the overall system given n generators:

$$\begin{aligned}
\dot{\boldsymbol{\psi}}_1 &= (\mathbf{K}(\Omega_1) + \mathbf{R}_1 \mathbf{X}_1^{-1}) \boldsymbol{\psi}_1 + \mathbf{E}\mathbf{u}_{g1} + \mathbf{b} u_{f1} \\
\dot{\boldsymbol{\psi}}_2 &= (\mathbf{K}(\Omega_2) + \mathbf{R}_2 \mathbf{X}_2^{-1}) \boldsymbol{\psi}_2 + \mathbf{E}\mathbf{u}_{g2} + \mathbf{b} u_{f2} \\
&\vdots
\end{aligned}$$

$$
\begin{aligned}
\dot{\boldsymbol{\psi}}_n =& (\mathbf{K}(\Omega_n) + \mathbf{R}_n\mathbf{X}_n^{-1})\boldsymbol{\psi}_n + \mathbf{E}\mathbf{u}_{gn} + \mathbf{b}u_{fn} \\
\dot{\Omega}_1 =& \frac{1}{T_{a1}}(T_{m1} - (\mathbf{G}\psi_1)^T\mathbf{H}\mathbf{G}\mathbf{X}_1^{-1}\boldsymbol{\psi}_1) \\
\dot{\Omega}_2 =& \frac{1}{T_{a2}}(T_{m2} - (\mathbf{G}\psi_2)^T\mathbf{H}\mathbf{G}\mathbf{X}_2^{-1}\boldsymbol{\psi}_2) \\
&\vdots \\
\dot{\Omega}_n =& \frac{1}{T_{an}}(T_{mn} - (\mathbf{G}\psi_n)^T\mathbf{H}\mathbf{G}\mathbf{X}_n^{-1}\boldsymbol{\psi}_n) \\
\Delta\dot{\delta}_2 =& \omega_N(\Omega_2 - \Omega_1) \\
&\vdots \\
\Delta\dot{\delta}_n =& \omega_N(\Omega_n - \Omega_1) \\
\dot{T}_{m1} =& \frac{1}{T_{DE1}}(-T_{m1} + z_1) \\
\dot{T}_{m2} =& \frac{1}{T_{DE2}}(-T_{m2} + z_2) \\
&\vdots \\
\dot{T}_{mn} =& \frac{1}{T_{DEn}}(-T_{mn} + z_n)
\end{aligned} \tag{73}
$$

where the vector $\mathbf{u}_{gi}$ is a function $\mathbf{u}_{gi}(\boldsymbol{\psi}_1, ..\boldsymbol{\psi}_n, \Delta\delta_2, ..., \Delta\delta_n)$ as given below:

$$\mathbf{u}_{g1} = \mathbf{Z}(\mathbf{w})(\mathbf{G}\mathbf{X}_1^{-1}\boldsymbol{\psi}_1 + \Phi(\Delta\delta_2)\mathbf{G}\mathbf{X}_2^{-1}\boldsymbol{\psi}_2 + \ldots + \Phi(\Delta\delta_n)\mathbf{G}\mathbf{X}_n^{-1}\boldsymbol{\psi}_n) \tag{74}$$

$$\mathbf{u}_{g2} = \Phi^T(\Delta\delta_2)\mathbf{u}_{g1} \tag{75}$$

$$. \tag{76}$$

$$. \tag{77}$$

$$. \tag{78}$$

$$\mathbf{u}_{gn} = \Phi^T(\Delta\delta_2)\mathbf{u}_{gn} \tag{79}$$

where $\mathbf{w} = [P_Z, Q_Z, P_S, Q_S]$ is 4 disturbance inputs given by the equations in the previous section, depending on selected motor and converter type. The outputs used by the PID controllers are the generator speeds $(\Omega_1, ..., \Omega_n)$ and the busbar voltage $(|\mathbf{u}_{g1}|)$. Define the following vectors:

$$\mathbf{u} = [u_{f_1}, \ldots, u_{f_n}, z_1, \ldots, z_n]^T$$

that is $2n$ manipulated inputs.

$$\mathbf{x} = [\boldsymbol{\psi}_1, \boldsymbol{\psi}_2, \ldots, \boldsymbol{\psi}_n, \Omega_1, \Omega_2, \ldots, \Omega_n, \Delta\delta_2, \ldots, \Delta\delta_n, T_{m1}, \ldots, T_{mi}]$$

that is $8n - 1$ states. Then

$$\dot{\mathbf{x}} = \mathbf{A}\mathbf{x} + \mathbf{f}(\mathbf{x}) + \mathbf{g}(\mathbf{x}, \mathbf{w}) + \mathbf{B}\mathbf{u} \tag{80}$$

where:

$$\mathbf{A} = \begin{bmatrix}
\mathbf{R}_1\mathbf{X}_1^{-1} & 0 & . & 0 & 0 & 0 & . & 0 & 0 & . & 0 & 0 & 0 & . & 0 \\
0 & \mathbf{R}_2\mathbf{X}_2^{-1} & . & 0 & 0 & 0 & . & 0 & 0 & . & 0 & 0 & 0 & . & 0 \\
. & . & . & 0 & 0 & 0 & . & 0 & 0 & . & 0 & 0 & 0 & . & 0 \\
0 & 0 & . & \mathbf{R}_n\mathbf{X}_n^{-1} & 0 & 0 & . & 0 & 0 & . & 0 & 0 & 0 & . & 0 \\
0 & 0 & . & 0 & 0 & 0 & . & 0 & 0 & . & 0 & \frac{1}{T_{a1}} & 0 & . & 0 \\
0 & 0 & . & 0 & 0 & 0 & . & 0 & 0 & . & 0 & 0 & \frac{1}{T_{a2}} & . & 0 \\
. & . & . & . & . & . & . & . & . & . & . & . & . & . & 0 \\
0 & 0 & . & 0 & 0 & 0 & . & 0 & 0 & . & 0 & 0 & 0 & 0 & \frac{1}{T_{an}} \\
0 & 0 & . & 0 & -\omega_N & \omega_N & . & 0 & 0 & . & 0 & 0 & 0 & 0 & 0 \\
. & . & . & . & . & . & . & . & . & . & . & . & . & . & . \\
0 & 0 & . & 0 & -\omega_N & 0 & . & \omega_N & 0 & . & 0 & 0 & 0 & 0 & 0 \\
0 & 0 & . & 0 & 0 & 0 & . & 0 & 0 & . & 0 & -\frac{1}{T_{DE1}} & 0 & 0 & 0 \\
0 & 0 & . & 0 & 0 & 0 & . & 0 & 0 & . & 0 & 0 & -\frac{1}{T_{DE2}} & 0 & 0 \\
. & . & . & . & . & . & . & . & . & . & . & . & . & . & . \\
0 & 0 & . & 0 & 0 & 0 & . & 0 & 0 & . & 0 & 0 & 0 & 0 & -\frac{1}{T_{DEn}}
\end{bmatrix}$$

$$\mathbf{f}(\mathbf{x}) = \begin{bmatrix}
\mathbf{K}(\Omega_1) \\
\mathbf{K}(\Omega_2) \\
. \\
\mathbf{K}(\Omega_n) \\
(\mathbf{G}\psi_1)^T\mathbf{H}\mathbf{G}\mathbf{X}_1^{-1}\boldsymbol{\psi}_1 \\
(\mathbf{G}\psi_2)^T\mathbf{H}\mathbf{G}\mathbf{X}_2^{-1}\boldsymbol{\psi}_2 \\
. \\
(\mathbf{G}\psi_n)^T\mathbf{H}\mathbf{G}\mathbf{X}_n^{-1}\boldsymbol{\psi}_n \\
0 \\
. \\
0 \\
0 \\
0 \\
. \\
0
\end{bmatrix}$$

$$\mathbf{g}(\mathbf{x}, \mathbf{w}) = \left[\mathbf{u}_{g1}, \mathbf{u}_{g1}, \ldots, \mathbf{u}_{gn}, 0, 0, . . , 0, 0, . . , 0, 0, 0, . . , 0\right]^T$$

5 SIMULATIONS

The model is implemented in Matlab-Simulink. A set of simulations is performed to investigate the model behavior. The following sections contain different simulation scenarios. Up to four generators are considered, and all plots are shown in p.u. values. The generators have equal parameters and the rating for one generator (60 Hz, 6000 kW) is chosen as reference for the p.u. system.

5.1 Simulations with Different Load Types

To investigate the dynamical behavior of the different load types (constant impedance and approximated constant power) two simulations are shown, one for each load type. As simulation case one generator is considered with an initial power output of 0.5 pu (that is 50% of full load) for both active and reactive power. A step in load demand from 0.5–0.7 is set for both active and reactive power at time 2s. Figures 6–9 show the results and comparison between the different load types. The constant impedance load type simulation is printed with dashed line and the constant power approximation load type is printed with solid line. The tuning of the PID controllers are done by trial and error on the simulation model, and a set of parameters are chosen which gives an acceptable performance in the sense of small overshoot and good damping of oscillations.

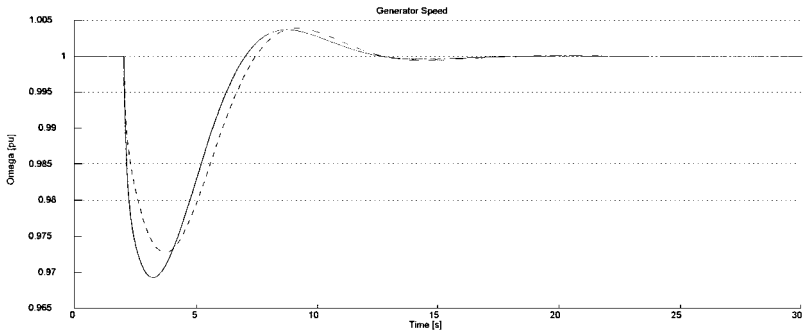

Fig. 6. Speed response for a step in active and reactive power demand. (- -) constant impedance load type and (—) appr. constant power load type.

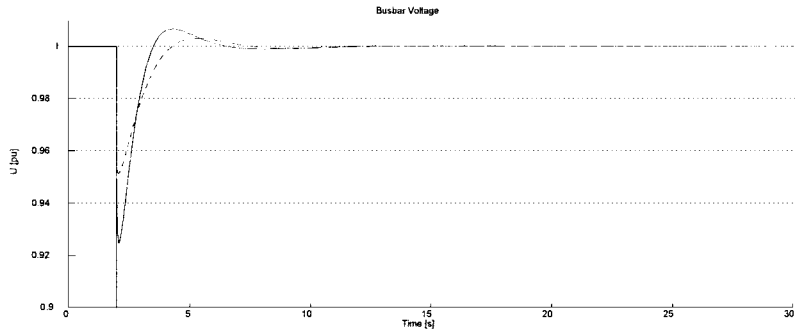

Fig. 7. Voltage response for a step in active and reactive power demand. (- -) constant impedance load type and (—) appr. constant power load type.

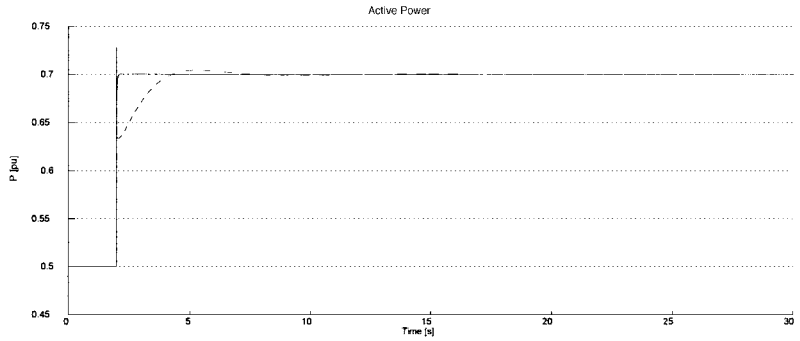

Fig. 8. Active power output for a step in active and reactive power demand. (- -) constant impedance load type and (—) appr. constant power load type.

5.2 Simulations With Two Generators

Figures 10–13 show a simulation with two generators and a step in total active and reactive power demand for the approximated constant power load type. This simulation is to show the behavior of the model with more than one generator supplying a common load. Slightly different parameters are used for the two generators, hence the active and reactive power outputs are slightly different. However the voltage and speeds of the generators are the same due to the synchronizing mechanism. Also stator resistance is set greater than zero, hence stator losses are included in the simulation showing greater power production than power consumption.

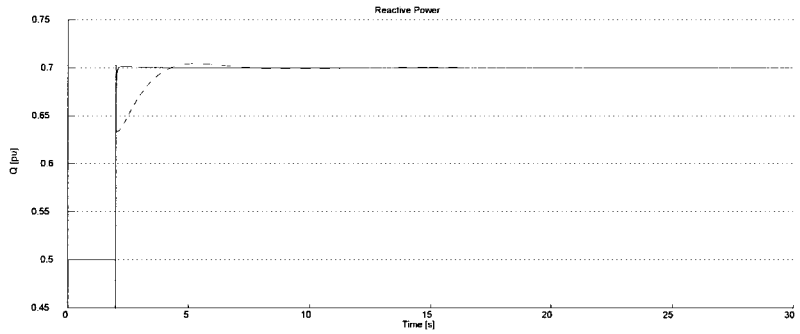

Fig. 9. Reactive power output for a step in active and reactive power demand. (- -) constant impedance load type and (—) appr. constant power load type.

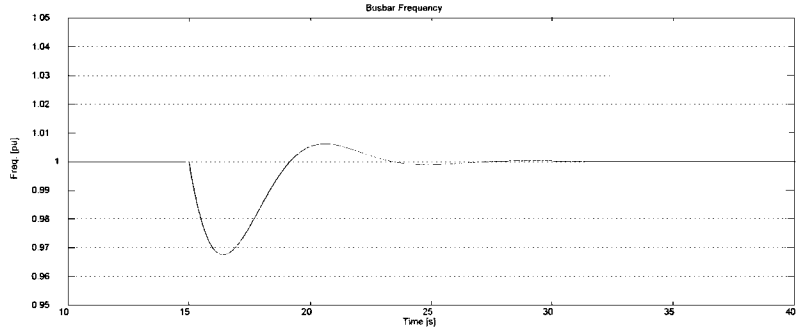

Fig. 10. Speed response for a step 1.0pu–1.2pu in both total active and reactive load demand.

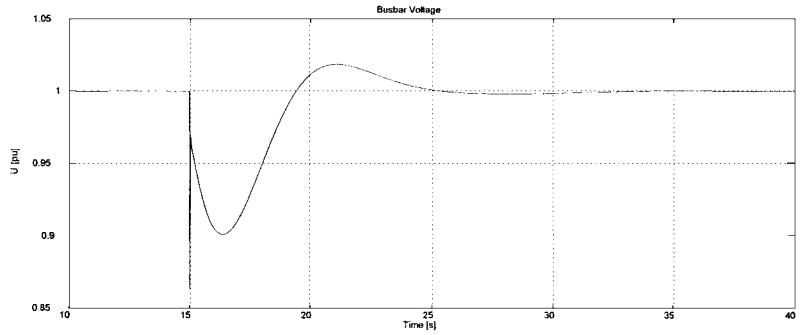

Fig. 11. Voltage respons for a step 1.0pu–1.2pu in both total active and reactive load demand.

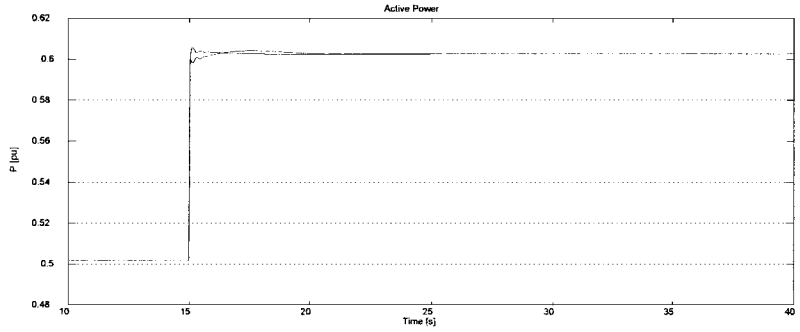

Fig. 12. Power outputs from generator 1 and 2 for a step 1.0pu–1.2pu in both total active and reactive load demand.

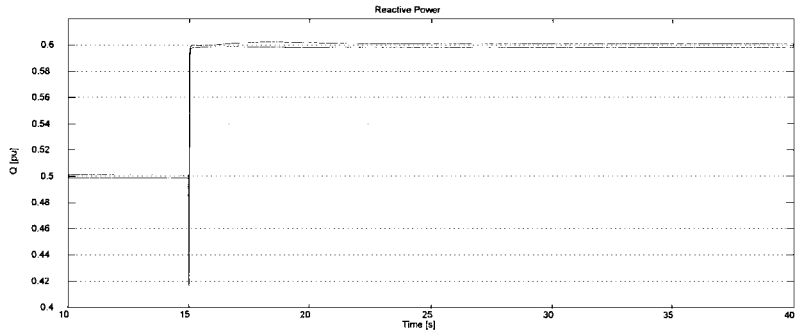

Fig. 13. Reactive power outputs of generator 1 and 2 for a step 1.0pu–1.2pu in both total active and reactive load demand.

5.3 Simulations With Total Model

In this section a simulation with the total model (including the power consumptions part) is shown. The performance of the power production system is simulated with a varying thrust demand at each propeller.

The simulated system contains 4 generators, three thruster drives and an aggregate domestic load model. Total load power from the thruster drives are shown with solid line in Figure 14, and the domestic load demand are shown with dashed line. Figures 15–18 show the simulation results. The following events appeared:

- *Start* : All generators were set to run in isochronous mode (equal load sharing).

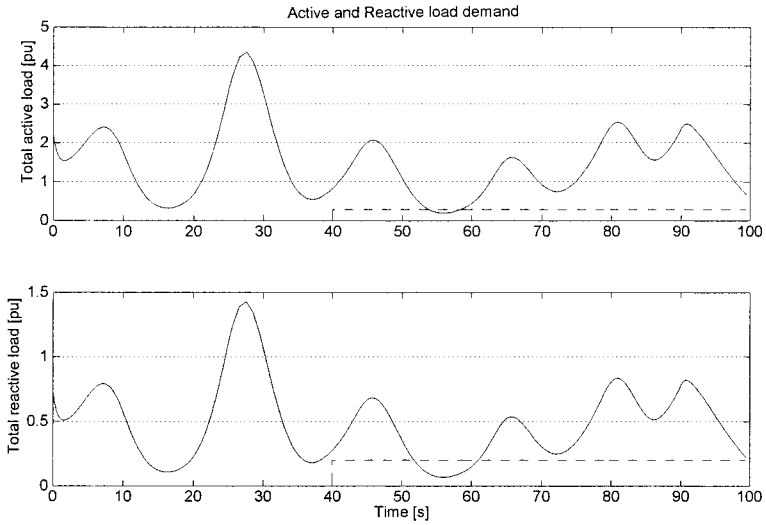

Fig. 14. Total load demand in pu for both active and reactive load (—) appr. constant power (thrusters), (- -) constant impedance (domestic loads).

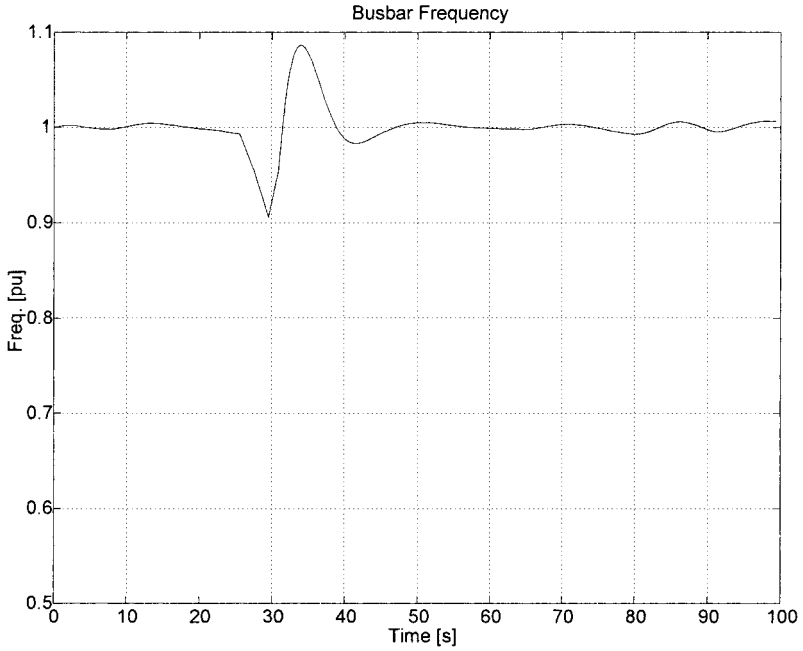

Fig. 15. Busbar frequency for the simulation case with total model.

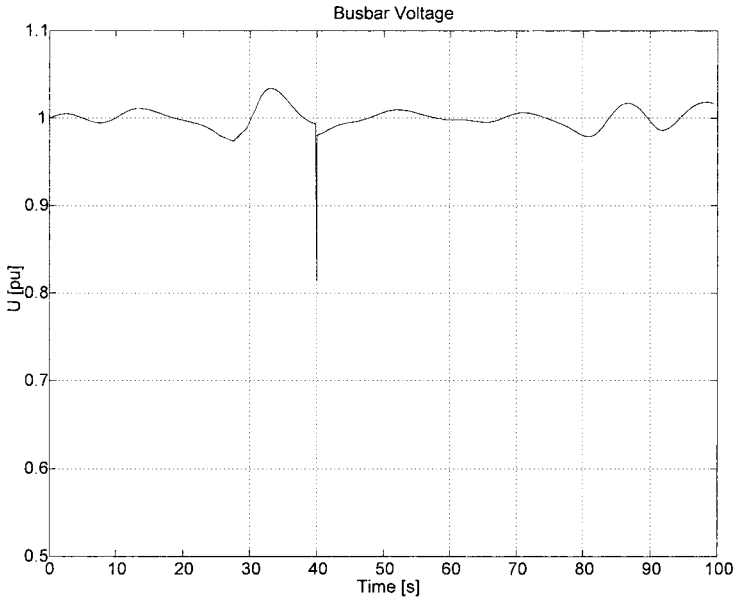

Fig. 16. Busbar voltage for simulation case with total model.

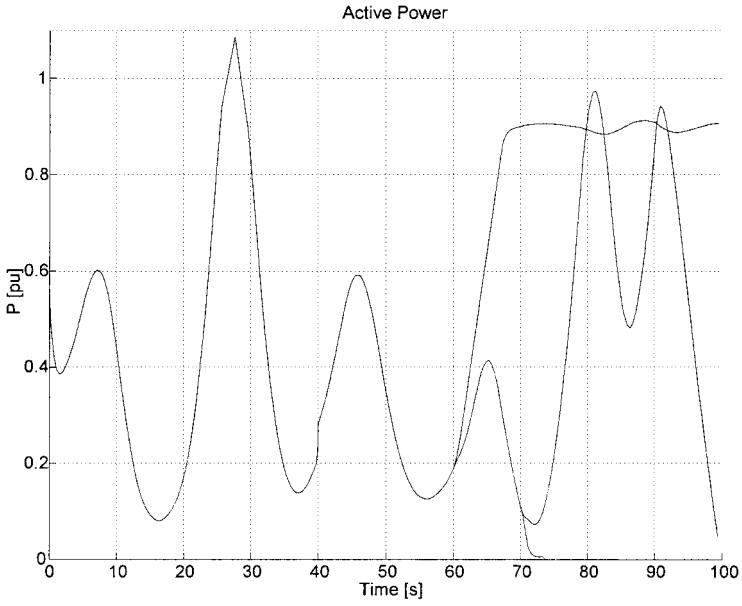

Fig. 17. Active power output from all the 4 generators.

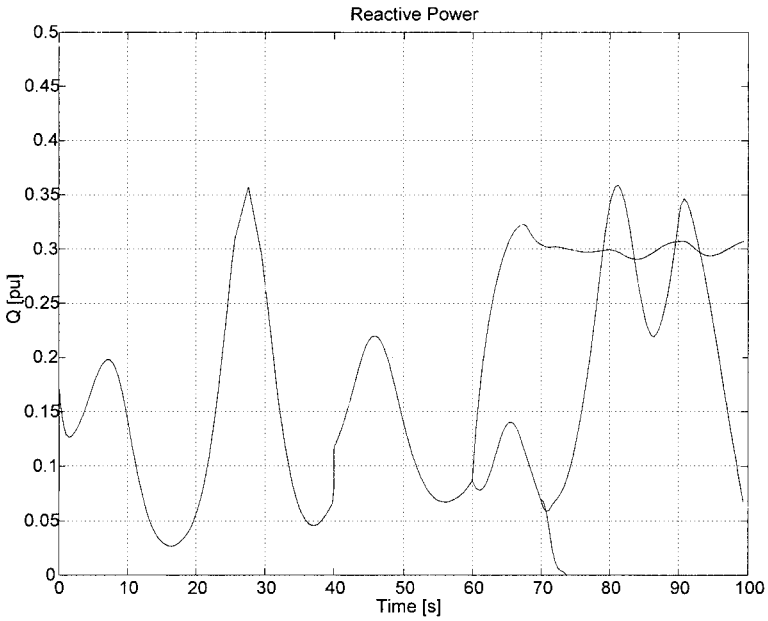

Fig. 18. Reactive power output for all 4 generators.

- *Time between 20 and 40 s.:* The total load were increasing high and rapid, hence speed governors saturated and a large frequency deviation occurred in this period
- *Time equals 40s:* A relative small (7,5% of total load) step in domestic load demand (both active and reactive). This had clearly most effect on the busbar voltage which is far more sensitive to steps in load changes than the frequency.
- *Time equals 60s:* One generator is set in droop mode, to take a constant power (0,9 pu in P and 0,3 pu in Q).
- *Time equals 70s:* One generator is shut down.

The last two generators are running with equal load sharing all the time.

6 CONCLUDING REMARKS

In this article a mathematical model of a marine power system consisting of diesel-generators, thruster drives and other loads is presented. The model is developed for the purpose of simulation and control design.

Most attention has been paid to the power generation system where advanced dynamical models are included. For the thruster drives stationary equations describing the power demand has been used. An aggregate load model is representing the other loads.

Emphasis has been paid to get a correct representation of diesel-generators working together with no external stiff network. Further the model was written in compact vector form as a non-linear state space model. The purpose of this is to be able to introduce new control technologies to investigate and improve performance and fuel-efficiency in future work.

The simulations show how the system responds to changes in thruster loads.

REFERENCES

1. IMarE, (ed.): Electric Propulsion, The Effective Solution? The Institute of Marine Engineers, 1995.
2. IMarE, (ed.): All Electric Ship, Eveloping Benefits for Maritime Applications. The Institute of Marine Engineers, 1998.
3. NIF, (ed.): 1st International Conference on Diesel Electric Propulsion—a Cost Effective Solution. Norwegian Society of Chartered Engineers, 1996.
4. NIF, (ed.): 2nd International Conference on Diesel Electric Propulsion. Norwegian Society of Chartered Engineers, 1998.
5. Hopkins, J.W. Fantasy and reality. Trans IMarE 103 (1991), pp.193–220.
6. Hill, W.A., Creelman, G. and Misschke, L.: Control Strategy for an Icebreaker Propulsion System. IEEE Trn. Industry Appl. 28 (1992), pp.887–892.
7. Schriek, D. and deNijs, J.W.: Royal Netherlands Navy M Class Frigate: Integrated Monitoring and Control System and Electrical Installation. Trans IMarE 103 (1991), pp.269–291.
8. Ådnanes, A.K. and Risdal, E.: Faster to the Field with a Better Total Solution Using Unified Power and Automation Package. In: IMECE '97, Shanghai, May 1997.
9. Doerry, N.H. and Davis, J.C.: Integrated Power System for Marine Application. Naval Eng. J. (1994), pp.77–90.
10. Tinney, M.D. and Hensler, J.: Efficiency and Power Density Improvements in Electric Propulsion Systems. In: INEC 94 Cost Effective Maritime Defence. The Institute of Marine Engineers, 1994, pp.175–183.
11. Parker, D.S. and Hodge, C.G.: The Electric Warship. Power Eng. J. pp.5–13.
12. Smith, K.S., Yacamini, R. and Williamson, A.C.: Cycloconverter Drives for Ship Propulsion. Trans IMarE 105 (1993), pp.23–52.
13. Sallabank, P.H. and Whitehead, A.J.: The Practical Application of Modern Simulation Tools Throughout the Design and Trials of a Diesel Electric Propulsion System. Trans IMarE 107 (1995), pp.101–117.
14. Smith, J.R., Stronach, A.F. and Mitchell, A.T.: Prediction of the Electrical System Behaviour of Special Purpose Vessels. Trans IMarE 97 (1985), pp.11–22.

15. Ordys, A.W. Pike, A.W. Johnson, M.A. Katebi, R.M and Grimble, M.J.: Modelling and Simulation of Power Generation Plants. Advances in Industrial Control, Springer-Verlag, 1994.
16. Mariani, E. and Murthy, S.S.: Control of Modern Integrated Power Systems. Advances in Industrial Control, Springer-Verlag, 1997.
17. Rafian, M. Sterling, M.J.H. and Irving, M.R.: Real-Time Power System Simulation. In: IEE Proc. 134 (1987), pp.206–223.
18. Kwatny, H.G., Maffezzoni, C., Paserba, J.J. Sanchez-Gasca, J.J. and Larsen, E.V.: The Control Handbook. CRC Press, 1996, ch. 79: Control of Electrical Power. pp.1453–1495.
19. Wang, Y. and Hill, D.J.: Robust Nonlinear Coordinated Control of Power Systems. Automatica 32(4) (1996), pp.611–618.
20. Lu, Q. and Sun, Y.: Nonlinear Stabilizing Control of Multimachine Systems. IEEE Trans Power Sys 4(1) (1989), pp. 236–241.
21. Fossen, T.I., Guidance and Control of Ocean Vehicles. Wiley, 1994.
22. Bühler, H.: Einführung in Die Theorie Geregelter Drehstrom-Antriebe. Birkhauser Verlag Basel, 1977.
23. Price, W.W., Chiang, H.D., Clark, H.K., Concordia, C., Lee, D.C., Hsu, J.C., Ihara, S., King, C.A., Lin, C.J., Mansour, Y., Srinivasan, K., Taylor, C.W. and Vaahedi, E.: Load Representation for Dynamic Performance Analysis. IEEE Task Force Report. IEEE Trans. Power Sys 8(2) (1993), pp.472–482.
24. Fitzgerald, A.E., Kingsley, C. and Umans, S.D.: Electric Machinery . McGraw-Hill, 5th (ed.), 1992.
25. Mohan, N. Undeland, T.M. and Robbins, W.P.: Power Electronics: Converters, Applications and Design. Wiley, 1989.
26. Wetterhus, T.M.: Comparison of fuel consumption in electric propulsion systems with fixed speed and variable speed thruster motors. Master's thesis, Norwegian Institute of Technology, Department of Electrical Power Engineering, 1995.